Published in final edited form as:
J Neurophysiol. 2004 September ; 92(3): 1558–1565. doi:10.1152/jn.00300.2004.

Excitation of Cerebellar Interneurons by Group I Metabotropic Glutamate Receptors

Movses H. Karakossian and **Thomas S. Otis**
Department of Neurobiology, University of California Medical Center, Los Angeles, California 90095-1763

Abstract

Cerebellar basket and stellate neurons (BSNs) provide feed-forward inhibition to Purkinje neurons (PNs) and thereby play a principal role in determining the output of the cerebellar cortex. During low-frequency transmission, glutamate released at parallel fiber synapses excites BSNs by binding to AMPA receptors; high-frequency transmission also recruits *N*-methyl-D-aspartate (NMDA) receptors. We find that, in addition to these ligand-gated receptors, a G-protein–coupled glutamate receptor subtype participates in exciting BSNs. Stimulation of metabotropic glutamate receptor 1α (mGluR1α) with the mGluR agonist (*RS*)-3,5-dihydroxyphenylglycine (DHPG) leads to an increase in spontaneous firing of BSNs and indirectly to an increase in the frequency of spontaneous inhibitory postsynaptic currents (sIPSCs) recorded in PNs. Under conditions in which ligand-gated glutamate receptors are blocked, parallel fiber stimulation generates a slow excitatory postsynaptic current (EPSC) in BSNs that is inhibited by mGluR1α-selective antagonists. This slow EPSC is capable of increasing BSN spiking and indirectly increasing sIPSCs frequency in PNs. Our findings reinforce the idea that distinct subtypes of glutamate receptors are activated in response to different patterns of activity at excitatory synapses. The results also raise the possibility that mGluR1α-dependent forms of synaptic plasticity may occur at excitatory inputs to BSNs.

INTRODUCTION

The output of the cerebellar cortex is transmitted entirely by action potentials carried along axons of Purkinje neurons (PNs). Because PNs have a high level of spontaneous activity in the absence of synaptic input (Häusser and Clark 1997), synaptic inhibition of PNs has a critical influence on the output of the cerebellar cortex. Two types of cerebellar interneurons, basket and stellate neurons (BSNs), inhibit PNs in a feed-forward manner. Each of these cell types is excited by glutamate which is released from parallel fibers; the glutamate binds to AMPA and *N*-methyl-D-aspartate (NMDA) subtypes of glutamate receptors (Barbour et al. 1994; Carter and Regehr 2000; Clark and Cull-Candy 2002). Recent evidence suggests that AMPA and NMDA receptors are activated in response to different frequencies of presynaptic activity, with NMDA receptors requiring bursts of high-frequency input (Clark and Cull-Candy 2002).

At many excitatory synapses, glutamate also binds to G-protein–coupled glutamate receptors (mGluRs) located on the postsynaptic membrane. Eight genes encoding mGluRs are known and have been classified into three groups (Pin and Duvoisin 1995). The group I mGluRs (mGluR1 and mGluR5) are distinguished from other mGluRs in that they are coupled to phospholipase C and are typically found in postsynaptic membranes. In the cerebellar cortex, a splice variant of mGluR1 termed mGluR1α is located on PNs at the peripheries of parallel

Address for reprint requests and other correspondence: T. S. Otis, Dept. of Neurobiology, UCLA Medical Center, 650 Charles Young Dr., Box 951763, Los Angeles, CA 90095-1763 (E-mail: E-mail: otist@ucla.edu)..

fiber and climbing fiber synapses (Baude et al. 1993; Lujan et al. 1996; Nusser et al. 1994; Petralia et al. 1997). At these synapses, mGluR1α gives rise to a slow phase of the excitatory postsynaptic current (Batchelor et al. 1994; Brasnjo and Otis 2001; Dzubay and Otis 2002; Hirono et al. 1998; Tempia et al. 1998) and triggers intracellular calcium release from IP_3-sensitive stores (Dzubay and Otis 2002; Finch and Augustine 1998; Takechi et al. 1998). Mice deficient in mGluR1α are ataxic and lack mGluR-dependent forms of synaptic plasticity (Aiba et al. 1994; Conquet et al. 1994; Ichise et al. 2000).

Group I mGluRs are also expressed postsynaptically by BSNs (Hamori et al. 1996), although much less is known of their function. A previous study using a broad spectrum mGluR agonist reported multiphasic effects on synaptic inhibition and BSN excitability (Llano and Marty 1995) and concluded that different subtypes of mGluRs located on pre-synaptic terminals and in somatodendritic regions influence local synaptic circuits.

We found that activation of mGluR1α leads to a robust depolarization of BSNs. This depolarization in turn triggers bursts of inhibitory synaptic currents in PNs. Stimulation of parallel fibers mimics the effects of mGluR agonists, showing that physiological activation of these receptors increases inhibition of PNs. Activation of mGluR1α on BSNs is likely to provide phasic, long-duration increases in PN inhibition. These receptors may also contribute to plasticity of inhibitory circuitry in the cerebellar cortex (Jorntell and Ekerot 2002; Rancillac and Crepel 2004).

METHODS

Brain slice preparation

Parasagittal cerebellar slices were prepared as previously described (Otis et al. 1997) in accordance with an animal protocol approved by the UCLA Chancellor's ARC. The cerebellum was removed from the cranium of a 12- to 16-day-old Sprague-Dawley rat, mounted on an agar support, and sectioned parasagittally using a vibrotome (Leica VT-1000) while submerged in cold (<4°C) artificial cerebrospinal fluid (ACSF). Following sectioning, the 300-μm slices were stored in 35°C ACSF for 30 min and brought to room temperature for subsequent electrophysiological experiments.

Solutions

The ACSF used during sectioning, storage, and electrophysiological recordings was saturated with 95% O_2-5% CO_2 and consisted of the following (in mM): 119 NaCl, 26 $NaHCO_3$, 11 glucose, 2.5 KCl, 2.5 $CaCl_2$, 1.3 $MgCl_2$, and 1 NaH_2PO_4. Specific drugs were added during electrophysiological recordings as indicated. In whole cell patch-clamp recordings from PNs, the pipette solution consisted of the following (in mM): 140 CsCl, 10 HEPES, 0.2 EGTA, 4 $MgCl_2$, 4 ATP, 0.4 GTP, and 5 *N*-[2,6-dimethylphenylcarbamoylmethyl] triethylammonium bromide (QX-314). For whole cell recordings from BSNs, pipettes contained (in mM) 140 KMeSO, 10 HEPES, 1 EGTA, 2 $MgCl_2$, 0.1 $CaCl_2$, 4 ATP, and 0.4 GTP or 140 mM CsMeSO, 10 HEPES, 10 BAPTA, 2 $MgCl_2$, 5 $CaCl_2$, 4 ATP, and 0.4 GTP. In loose-patch (15–200 MΩ) extracellular recordings, the extracellular solution was used as pipette solution. The drugs used in electrophysiological recordings were of the following concentrations: either 20 μM 6,7-dinitroquinoxaline-2,3-[1*H*,4*H*]-dione (DNQX) or (in synaptic stimulation experiments) 50 μM 2,3-dioxo-6-nitro-1,2,3,4-tetrahydrobenzo[f]quinoxaline-7-sulfonamide (NBQX), 5 μM [*RS*]-3-[2-carboxypiperazin-4-yl]-propyl-1-phosphonic acid (CPP), 100 μM picrotoxin (PTX), 500 nM TTX, 50–100 μM $CdCl_2$, and 2–4 μM 1-[2,4-dichlorophenyl]-5-[4-iodophenyl]-4-methyl-*N*-4-morpholinyl-1*H*-pyrazole-3-carboxamide (AM281), or 2–4 μM *N*-(piperidin-1-yl)-5-(4-iodophenyl)-1-(2,4-dichlophenyl)-4-methyl-1*H*-pyrazole-3-carboxamide (AM251), 100–200 μM (*S*)-(+)-α-amino-4-carboxy-2-methylbenzeneacetic acid

(LY367385), 100–200 μM 7-(hydroxyimino)cyclopropa[b]chromen-1a-carboxylate ethyl ester (CPCCOEt), 1 μM 2-methyl-6-[phenylethynyl]pyridine hydrochlo-ride (MPEP), 50 μM (*RS*)-3,5-dihydroxyphenylglycine (DHPG), 1 mM [*RS*]-2-chloro-5-hydroxyphenylglycine (CHPG), and 100 μM D,L-*threo*-β-benzyloxyaspartate (TBOA).

Electrophysiology

PN and BSN cell bodies were visualized using an upright microscope with a 40× water immersion lens and equipped with an infrared-DIC enhancement. Whole cell voltage-clamp recordings from PNs were performed using an Axopatch 200B amplifier (Axon Instruments, Foster City, CA). Electrophysiological recordings were filtered at 1 kHz and digitized at 2–4 kHz. Pipettes were typically 1.4–2.0 MΩ for recordings from PNs and 3.0–3.5 MΩ for BSNs. Series resistances were not compensated but did not exceed 20 MΩ for PNs and 30 MΩ for BSNs. Whole cell patch-clamp recordings from PNs were made in ACSF containing DNQX or NBQX, CPP, and AM281 or AM251; in whole cell recordings from BSNs, PTX was added to the latter solution. In Fig. 2, TTX and $CdCl_2$ were also added to the ACSF. Loose-patch extracellular recordings from BSNs were performed in an ACSF solution containing DNQX or NBQX, CPP, PTX, and AM281. Agonists for mGluR1 and mGluR5, DHPG and CHPG, respectively, were pressure applied (1- to 2-s duration, 1–5 psi) using a picospritzer (Parker Hannifin, Fairfield, NJ) connected to a glass pipette. Antagonists for mGluR1 and mGluR5, LY367385/CPCCOEt and MPEP, respectively, were bath-applied. All drugs were purchased from Tocris Cookson (Ballwin, MO), with the exception of PTX, $CdCl_2$, BAPTA (Sigma-Aldrich, St. Louis, MO), and TTX (Accurate Chemicals, Westbury, NY). In synaptic stimulation experiments, parallel fibers were activated by applying a train of 10 constant current pulses (50–200 μA, 100 μs) at 100 Hz using a bipolar glass electrode (theta pipette, 0.5–1.0 MΩ) placed in the molecular layer surrounding BSNs. For clarity, the electrical stimulus artifacts have been removed from traces displayed in Figs. 6 and 7. Unless otherwise noted, all recordings were performed at a range of 20–24°C, and all holding potentials in whole cell recordings were between −70 and −80 mV.

Data analysis and statistics

Data analysis was performed using routines written in Igor Pro 3.13 (Wavemetrics, Lake Oswego, OR). Statistical significance was established using Student's *t*-test. *P* values are reported in the text and unless otherwise indicated represent comparisons to a baseline value of 100%.

RESULTS

DHPG-induced spontaneous inhibitory postsynaptic currents are due to the activation of mGluR1α

Recent findings in cerebellum and hippocampus indicate that activation of group I mGluRs can trigger cannabinoid production in postsynaptic neurons, leading to a retrograde form of presynaptic inhibition (Brown et al. 2003; Maejima et al. 2001; Varma et al. 2001). In cerebellum, such mGluR-cannabinoid signaling can inhibit parallel or climbing fiber evoked EPSCs (Brown et al. 2003; Maejima et al. 2001), but it is not known if a similar mGluR-initiated mechanism can inhibit release of GABA from inhibitory inputs to PNs. To study the effects of group I mGluR agonists in the absence of potentially opposing cannabinoid-mediated inhibition, all of the following experiments have been conducted in a cannabinoid receptor antagonist (see METHODS).

Spontaneous IPSCs were recorded from individual PNs in the presence of AMPA, NMDA, and cannabinoid receptor antagonists, whereas group I mGluRs were activated by pressure pipette application of DHPG in the vicinity of PN dendrites. As shown in Fig. 1*A*, each DHPG

application elicited a slow inward current and superimposed on this slow current was a burst, lasting several seconds in duration, of fast phasic currents. Subsequent experiments, shown in Fig. 2, confirm that these bursts of phasic currents are mediated by $GABA_A$ receptors and they are hereafter referred to as spontaneous inhibitory postsynaptic currents (sIPSCs). Average results from several PNs indicated that, in the absence of mGluR1α antagonists, significant increases in sIPSC amplitude (180 ± 20%, $n = 7$; $P < 0.005$) and frequency (213 ± 18%, $n = 11$; $P < 0.01$; Fig. 1*C*) were elicited by DHPG application. The effects of mGluR activation on sIPSC frequency have a more straightforward interpretation than those on sIPSC amplitude, which depend on both pre- and postsynaptic factors. For this reason, we have focused our analyses on changes in sIPSC frequency, which as will be shown below, can be attributed solely to presynaptic factors.

To discriminate whether DHPG-initiated bursts of sIPSCs are due to the activation of mGluR1α or mGluR5, we tested whether the bursts were sensitive to mGluR1α-selective antagonists. The effects of a competitive (LY367385) and a non-competitive (CPCCOEt) antagonist of mGluR1α were examined. As expected (Batchelor et al. 1994; Brasnjo and Otis 2001; Dzubay and Otis 2002; Hirono et al. 1998; Tempia et al. 1998), both antagonists inhibited the slow, mGluR-mediated current in PNs (cf. Fig. 1, *A* and *B*). Both antagonists also prevented DHPG-induced increases in sIPSC frequency (LY367385, $n = 5$; $P = 0.78$ compared with baseline frequency; CPCCOEt, $n = 6$; $P = 0.90$ compared with baseline frequency). However, the two antagonists also had unexpected effects as LY367385 increased baseline sIPSC frequency moderately to 138 ± 40% of control, whereas CPCCOEt reduced it to 79 ± 3% (Fig. 1*C*). It should be noted that these seemingly opposing effects of the antagonists on baseline activity were consistently observed in a variety of related experiments (see Figs. 3, 5, and 7). Taken together, the results imply that activation of mGluR1α excites local inhibitory interneurons, leading to an increased inhibition of PNs.

DHPG-induced sIPSCs are presynaptic in origin

In principle, the increase in sIPSC activity in PNs could be caused by excitation of presynaptic GABAergic neurons or by a postsynaptic increase in $GABA_A$ receptor sensitivity. Considering that an increase in $GABA_A$ receptor sensitivity has been reported in response to co-application of mGluR agonists and brain-derived neurotrophic factor (BDNF) to PNs (Boxall 2000), we tested whether, under our experimental conditions, postsynaptic changes in $GABA_A$ receptor sensitivity could contribute to the observed effects. To limit passive and active excitation of BSN terminals (Glitsch and Marty 1999), mIPSCs were measured in the presence of 500 nM TTX and 50–100 μM $CdCl_2$. Pressure-pipette application of DHPG gave rise to the slow mGluR-mediated inward current; however, no elevation in mIPSC amplitude or frequency was observed (Fig. 2, *A* and *C*; $n = 7$), consistent with previous experiments involving only DHPG (Boxall 2000). Subsequent application of 100 μM PTX to the bathing solution (Fig. 2*B*) abolished the mIPSCs and left the slow mGluR-mediated current, confirming that all synaptic events were $GABA_A$ receptor-mediated. These results confirm that the IPSC activity is due to activation of $GABA_A$ receptors and rule out the possibility that postsynaptic changes contribute to the increased sIPSC activity described in Fig. 1.

DHPG-induced sIPSCs are not due to activation of mGluR5

The findings described above are consistent with the hypothesis that mGluR1α is solely responsible for DHPG-evoked increases in sIPSC frequency. However, another group I mGluR, mGluR5, has been reported to be expressed in a population of neurons whose soma and dendrites reside in the molecular layer (Negyessy et al. 1997). To determine the level of involvement of mGluR5, we evaluated the effects of mGluR5-specific reagents. We tested whether the mGluR5-specific antagonist, MPEP, could inhibit responses elicited by pressure application of DHPG (Fig. 3). Normalized, averaged results shown in Fig. 3*D* indicated that

MPEP had no effect on peak frequency in response to DHPG (319 ± 80% in the absence and 326 ± 64% in the presence of MPEP; $P = 0.95$). Supporting the results shown in Fig. 1, addition of LY367385 completely antagonized the DHPG-evoked increases not blocked by MPEP (Fig. 3, *C* and *D*).

A second experiment provided more evidence that mGluR5 is not involved. Instead of applying DHPG, the specific mGluR5 agonist CHPG was pressure applied (Fig. 4*A*). This agonist had no significant effect on sIPSC frequency (Fig. 4; $n = 6$; $P = 0.22$). The CHPG and MPEP results indicate that mGluR1α but not mGluR5 is responsible for the DHPG-induced increases in sIPSC frequency observed from recordings in PNs.

Activation of mGluR1α induces action potentials in BSNs

Results presented to this point suggest that mGluR1α, located on BSN dendrites, couples to an excitatory conductance. To monitor the excitability of individual BSNs, their action potential firing rate was measured with loose-patch extracellular recordings. Figure 5*A* shows an extracellular action potential recording from a BSN to which DHPG was pressure-applied. In this BSN, DHPG increased the firing rate from a baseline rate of 7 Hz to a peak of 20 Hz (Fig. 5, *A* and *C*), and this increase was blocked by LY367385 (Fig. 5, *B* and *C*). Mean, normalized results from several BSNs indicated that DHPG induced an approximate threefold increase in action potential frequency (273 ± 52%; $n = 6$; $P < 0.01$; Fig. 5*D*), which was prevented by LY367385 ($n = 6$; $P = 0.58$). Consistent with the LY367385-induced elevation in sIPSC baseline frequency observed in PN recordings (Figs. 1 and 3), this compound increased baseline frequency of firing in BSNs. Mean baseline firing frequency, normalized to data obtained in the absence of LY367385, was 142 ± 14% ($n = 6$; Fig. 5*D*). These findings clearly indicate that activation of mGluR1α excites BSNs, explaining the bursts of sIPSCs observed in PNs. Moreover, the LY367385-induced increase in baseline sIPSC frequency in PNs and firing frequency of BSNs implies that this compound may act as a weak partial agonist at mGluR1α.

mGluRs on BSNs can be synaptically activated by parallel fiber inputs

Results presented in the previous section indicate that the activation of mGluR1α by exogenous agonists can depolarize BSNs. To assess whether synaptically released glutamate is capable of activating mGluR1α on BSNs, a series of synaptic experiments were undertaken. BSNs were targeted for whole cell recording based on their location in the molecular layer of the cerebellar cortex as well as on distinctive morphological features such as the presence of more than one primary dendrite. Once a whole cell recording was established from a candidate BSN, its input resistance was measured to unambiguously discriminate it from an ectopic PN. Input resistances ranged from 300 MΩ to 2 GΩ (840 ± 92 MΩ; $n = 29$), confirming these cells as BSNs (Carter and Regehr 2002; Häusser and Clark 1997). Interneurons in the molecular layer have been classified either as stellate or basket cells, although analysis of morphological criteria and cell body localization suggests a uniform population of interneurons (Sultan and Bower 1998). In the present study, the localization of the cell body within the molecular layer did not correlate with any of the physiological properties reported below, and therefore we treated BSNs as a homogenous group as has been done in previous physiological studies (Glitsch and Marty 1999; Häusser and Clark 1997; Kreitzer and Regehr 2002).

In the presence of $GABA_A$, AMPA, and NMDA receptor antagonists (see METHODS), BSNs were voltage clamped near −70 mV. Stimulation of parallel fibers with short trains (10 pulses at 100 Hz) gave rise to slow excitatory postsynaptic currents (EPSCs). Blocking glutamate uptake with TBOA (100 μM) enhanced net charge underlying these slow EPSCs by approximately fourfold (377 ± 89%; $n = 11$; $P < 0.01$; Fig. 6*D*), a pharmacological profile characteristic of mGluR1α-mediated synaptic signals in PNs (Brasnjo and Otis 2001;Dzubay and Otis 2002).

Moreover, the charge transfer by the slow EPSC was significantly reduced on addition of LY367385 (to 7.8 ± 3.3% of control; $n = 6$; $P < 0.01$; Fig. 6*D*) or CPCCOEt (to 10.5 ± 1.6%; $n = 5$; $P = 0.02$; Fig. 6*D*).

Compared with the peak amplitudes of AMPA receptor–mediated fast EPSCs in BSNs, slow mGluR-mediated EPSCs represent a small conductance. Even considering the high-input resistance of BSNs (Carter and Regehr 2002) and the slow time course of the conductance, it is unclear whether such mGluR-mediated EPSCs would be sufficient to excite BSNs. To establish whether activation of mGluRs on BSNs results in changes in their firing frequency, loose-patch, extracellular recordings were performed. Stimulation of parallel fiber inputs gave rise to an approximate threefold increase in action potential firing frequency (265 ± 18%; $n = 10$; $P < 0.01$; Fig. 7). These increases were blocked by LY367385 ($n = 8$; $P = 0.62$ compared with baseline frequency) or CPCCOEt ($n = 6$; $P = 0.63$ compared with baseline frequency), indicating that the excitation results from mGluR1α and is not due to direct stimulation of BSNs. As in previous experiments, baseline firing frequency was elevated (to 127 ± 24% of control; $n = 8$; Fig. 7*C*) in the presence of LY367385 and reduced (to 91 ± 9% of control; $n = 6$; Fig. 7*C*) in the presence of CPCCOEt. Two BSNs reversibly stopped firing in response to 100 μM CPCCOET and were excluded from analysis. Additional experiments using 200 μM CPCCOEt showed that BSN firing could be reversibly blocked with higher concentrations of this noncompetitive antagonist ($n = 6$; data not shown). These data indicate that glutamate released from parallel fiber synaptic terminals can elicit a slow EPSC in BSNs; although small in amplitude, this current is sufficient to depolarize BSNs and increase their firing rate.

DISCUSSION

Cerebellar interneurons are potently excited by mGluR1α

We find that, in addition to the two major subtypes of ionotropic glutamate receptors (AMPA and NMDA), mGluRs can also depolarize BSNs. Pharmacological experiments with selective agonists and antagonists for group I mGluRs indicate that mGluR1α excites BSNs, but that mGluR5, the other group I mGluR, is not capable of exciting BSNs. This is consistent with the localization patterns for mGluR1α and mGluR5 in cerebellar cortex; mGluR1α is found at parallel fiber contacts onto BSNs (Hamori et al. 1996), whereas mGluR5 is reported to be absent from BSNs, although it is expressed by a novel class of cells in the molecular layer (Berthele et al. 1998; Negyessy et al. 1997).

This evidence extends the observations of Llano and Marty, who showed that application of the broad-spectrum mGluR agonist *trans*-1-amino-1,3-cyclopentanediocarboxylic acid (ACPD) led to a multiphasic effect on IPSC frequency recorded in PNs. In their experiments, bath application of *trans*-ACPD led to rapid onset, rapidly recovering inhibition of sIPSCs superimposed with a slower onset, slowly recovering excitation of sIPSC frequency (Llano and Marty 1995). Based on these findings, they hypothesized that *trans*-ACPD is targeting at least two distinct sites. One is located on inhibitory presynaptic terminals and inhibits GABA release, whereas the other is located on somatodendritic membrane of BSNs and excites BSNs. The lack of specific mGluR agents available at the time prevented further dissection of these mechanisms. Using selective mGluR antagonists and agonists, we observe the excitatory component of this response to *trans*-ACPD. Furthermore, identification of the slow EPSC in BSNs confirms that they are directly excited by group I mGluRs. Although PNs give rise to a small number of recurrent collaterals (Palay and Chan-Palay 1974) and terminals formed by these collaterals could participate in generating sIPSCs in response to DHPG, the direct recordings from BSNs strongly implicate BSN inputs as the main source of mGluR-driven inhibition in PNs.

The experiments described here were carried out under conditions in which presynaptic cannabinoid receptors were blocked. Given the link between group I mGluRs and cannabinoid production, it is possible that both inhibitory and excitatory effects described in the study of Llano and Marty (1995) may be attributable to mGluR1*α*. This would arise if mGluR1*α* on PNs generated a presynaptic inhibition of GABA release while mGluR1*α* on BSNs excited inhibitory circuitry. Alternatively, cannabinoids produced by mGluR1 activation on either PNs or BSNs could slow the BSN firing rate (Kreitzer et al. 2002). Indeed, in preliminary experiments conducted in the absence of cannabinoid receptor antagonists, puffer pipette application of DHPG led to multiphasic bursts of sIPSCs (data not shown). Further experiments will be required to determine if mGluR1*α* by itself can account for the patterned inhibitory circuit activity observed in response to continuous activation of mGluRs.

Parallel fibers synaptically activate mGluR1α on BSNs

In PNs, it is well established that synaptic activation of mGluR1*α* at parallel fiber and climbing fiber inputs can generate a slow inward synaptic current (Batchelor et al. 1994; Brasnjo and Otis 2001; Dzubay and Otis 2002; Hirono et al. 1998; Tempia et al. 1998). Here we describe a similar slow inward synaptic current in BSNs elicited by delivering trains of stimuli to parallel fibers. This slow EPSC has several properties that resemble the slow EPSCs described in PNs: it is inhibited by the mGluR1*α*-selective antagonists LY367385 and CPCCOEt, inhibiting glutamate uptake enhances the slow EPSC, and kinetics of this current are similar to those described for PNs. Such mGluR-mediated EPSCs, although small, could have a significant effect on BSN membrane potential due to the high-input resistance of BSNs (Carter and Regehr 2002). Indeed, in the presence of antagonists for ionotropic glutamate receptors, parallel fiber activity is sufficient to transiently increase the firing rate of BSNs. This excitation is blocked by mGluR1*α*-selective antagonists, indicating that the additional spikes (BSNs are spontaneously active) are the result of mGluR activation.

Effects of mGluR1α antagonists on PN sIPSCs and BSN spiking

Agonist- and synaptically evoked excitation of BSNs was inhibited by the competitive and noncompetitive antagonists LY367385 and CPCCOEt, consistent with a role for mGluR1*α* in exciting cerebellar interneurons. However, these two antagonists also caused paradoxical effects on the baseline excitability of BSNs, with LY367385 exciting (131 ± 12% of control; $n = 17$; $P = 0.01$; see Figs. 5 and 7) and CPCCOEt depressing (87 ± 6% of control; $n = 9$; $P = 0.01$; see Fig. 7) BSN firing. Consistent with their distinct effects on BSN excitability, the antagonists also differentially affected sIPSC frequencies recorded from PNs, with CPCCOEt decreasing sIPSC frequency (76 ± 6% of control; $n = 6$; $P < 0.01$; see Fig. 1) and LY367385 increasing sIPSC frequency (155 ± 29% of control; $n = 10$; $P = 0.02$; see Figs. 1 and 3). The actions of CPCCOEt to depress BSN excitability are perhaps the most straightforward. We hypothesize that the noncompetitive antagonist is either inhibiting a tonic inward current caused by circulating low levels of glutamate or it is inhibiting an agonist-independent current (Ango et al. 2001). Given that the agonist-independent current is also dependent on mGluR1-interacting proteins in the homer family, future experiments involving over-expression of homer isoforms may be able to distinguish between the two possibilities.

As far as the excitatory actions of LY367385 are concerned, we favor the hypothesis that it is acting as a weak, partial agonist. This idea, rather than a nonspecific action unrelated to mGluR1*α*, is supported by the observation that CPCCOEt antagonizes the excitatory effect of LY367385 (87 ± 6% of control; $n = 7$; $P = 0.97$ compared with CPCCOEt alone). We attempted to detect changes in holding current that might be expected to occur in BSNs in response to the different antagonists but were unable to measure reliable effects. Given the high-input resistance of BSNs, very small currents, on the order of a few picoamperes, would be sufficient

to cause the changes in excitability seen in these experiments (Carter and Regehr 2002; Glitsch and Marty 1999).

Implications of mGluR activation for PN inhibition and synaptic plasticity within the cerebellar cortex

The slow time course of the mGluR EPSC should lead to a period of enhanced excitability in BSNs lasting for 2 or 3 s. Examples of extended increases in firing rate can be seen in Fig. 7. Such relatively prolonged periods of excitation should have important consequences for the output of PNs, because even single spikes in BSNs can temporarily silence the intrinsic firing of PNs (Häusser and Clark 1997). Pauses in PN firing are well correlated with movements, and it is these pauses that form the basis of the disinhibition hypothesis of cerebellar function (Eccles et al. 1967). Thus mGluR-mediated inputs to BSNs are in a pivotal position to influence the output of the cerebellar cortex.

A similar frequency-dependent excitation of BSNs has been attributed to extrasynaptic NMDA receptors (Clark and Cull-Candy 2002). The present form of synaptic excitation may differ in important respects. First, compared with NMDA receptor–mediated conductances, mGluR-mediated conductances are expected to show less voltage dependence, meaning that they would contribute to excitation near the resting membrane potential and would not require depolarization. Second, mGluR conductances have a significantly slower time course than NMDA-mediated conductances. Third, the presence of the mGluR EPSC implies that several second messenger cascades known to be linked to mGluRs will be initiated by parallel fiber activity. These additional signaling cascades may include IP_3-mediated intracellular calcium release (Finch et al. 1991; Takechi et al. 1998) as well as engagement of tyrosine kinases (Canepari and Ogden 2003). mGluR-mediated cascades play a central role in several forms of long term synaptic weakening (Bear and Abraham 1996; Hansel et al. 2001; Ito 2001), and recent findings have implicated mGluRs in a form of plasticity expressed at parallel fiber inputs to stellate cells (Rancillac and Crepel 2004). Further experiments will be required to determine whether mGluR1α receptors on BSNs are involved in the large scale, bi-directional modifications of parallel fiber receptive fields thought to occur in certain types of cerebellar learning (Jorntell and Ekerot 2002).

ACKNOWLEDGMENTS

We thank G. Brasnjo, Dr. Pratap Meera, and S. Smith for invaluable comments.

GRANTS

This study was supported by National Institute of Neurological Disorders and Stroke Grant NS-40449.

REFERENCES

Aiba A, Kano M, Chen C, Stanton ME, Fox GD, Herrup K, Zwingman TA, Tonegawa S. Deficient cerebellar long-term depression and impaired motor learning in mGluR1 mutant mice. Cell 1994;79:377–388. [PubMed: 7954803]

Ango F, Prezeau L, Muller T, Tu JC, Xiao B, Worley PF, Pin JP, Bockaert J, Fagni L. Agonist-independent activation of metabotropic glutamate receptors by the intracellular protein Homer. Nature 2001;411:962–965. [PubMed: 11418862]

Barbour B, Keller BU, Llano I, Marty A. Prolonged presence of glutamate during excitatory synaptic transmission to cerebellar Purkinje cells. Neuron 1994;12:1331–1343. [PubMed: 7912092]

Batchelor AM, Madge DJ, Garthwaite J. Synaptic activation of metabotropic glutamate receptors in the parallel fibre-Purkinje cell pathway in rat cerebellar slices. Neuroscience 1994;63:911–915. [PubMed: 7535396]

Baude A, Nusser Z, Roberts JD, Mulvihill E, McIlhinney RA, Somogyi P. The metabotropic glutamate receptor (mGluR1 alpha) is concentrated at perisynaptic membrane of neuronal subpopulations as detected by immunogold reaction. Neuron 1993;11:771–787. [PubMed: 8104433]

Bear MF, Abraham WC. Long-term depression in hippocampus. Annu Rev Neurosci 1996;19:437–462. [PubMed: 8833450]

Berthele A, Laurie DJ, Platzer S, Zieglgansberger W, Tolle TR, Sommer B. Differential expression of rat and human type I metabotropic glutamate receptor splice variant messenger RNAs. Neuroscience 1998;85:733–749. [PubMed: 9639268]

Boxall AR. GABAergic mIPSCs in rat cerebellar Purkinje cells are modulated by TrkB and mGluR1-mediated stimulation of Src. J Physiol 2000;524:677–684. [PubMed: 10790150]

Brasnjo G, Otis TS. Neuronal glutamate transporters control activation of postsynaptic metabotropic glutamate receptors and influence cerebellar long-term depression. Neuron 2001;31:607–616. [PubMed: 11545719]

Brown SP, Brenowitz SD, Regehr WG. Brief presynaptic bursts evoke synapse-specific retrograde inhibition mediated by endogenous cannabinoids. Nat Neurosci 2003;6:1048–1057. [PubMed: 14502290]

Canepari M, Ogden D. Evidence for protein tyrosine phosphatase, tyrosine kinase, and G-protein regulation of the parallel fiber metabotropic slow EPSC of rat cerebellar Purkinje neurons. J Neurosci 2003;23:4066–4071. [PubMed: 12764093]

Carter AG, Regehr WG. Prolonged synaptic currents and glutamate spillover at the parallel fiber to stellate cell synapse. J Neurosci 2000;20:4423–4434. [PubMed: 10844011]

Carter AG, Regehr WG. Quantal events shape cerebellar interneuron firing. Nat Neurosci 2002;5:1309–1318. [PubMed: 12411959]

Clark BA, Cull-Candy SG. Activity-dependent recruitment of extrasynaptic NMDA receptor activation at an AMPA receptor-only synapse. J Neurosci 2002;22:4428–4436. [PubMed: 12040050]

Conquet F, Bashir ZI, Davies CH, Daniel H, Ferraguti F, Bordi F, Franz-Bacon K, Reggiani A, Matarese V, Conde F, Collingridge GL, Crépel F. Motor deficit and impairment of synaptic plasticity in mice lacking mGluR1. Nature 1994;372:237–243. [PubMed: 7969468]

Dzubay JA, Otis TS. Climbing fiber activation of metabotropic glutamate receptors on cerebellar Purkinje neurons. Neuron 2002;36:1159–1167. [PubMed: 12495629]

Eccles, JC.; Ito, M.; Szentagothai, J. The Cerebellum as a Neuronal Machine. Springer-Verlag; New York: 1967.

Finch EA, Augustine GJ. Local calcium signalling by inositol-1,4,5-trisphosphate in Purkinje cell dendrites. Nature 1998;396:753–756. [PubMed: 9874372]

Finch EA, Turner TJ, Goldin SM. Calcium as a coagonist of inositol 1,4,5-trisphosphate-induced calcium release. Science 1991;252:443–446. [PubMed: 2017683]

Glitsch M, Marty A. Presynaptic effects of NMDA in cerebellar Purkinje cells and interneurons. J Neurosci 1999;19:511–519. [PubMed: 9880571]

Hamori J, Takacs J, Gorcs TJ. Immunocytochemical localization of mGluR1a metabotropic glutamate receptor in inhibitory interneurons of the cerebellar cortex. Acta Biol Hung 1996;47:181–194. [PubMed: 9123990]

Hansel C, Linden DJ, D'Angelo E. Beyond parallel fiber LTD: the diversity of synaptic and non-synaptic plasticity in the cerebellum. Nat Neurosci 2001;4:467–475. [PubMed: 11319554]

Häusser M, Clark BA. Tonic synaptic inhibition modulates neuronal output pattern and spatiotemporal synaptic integration. Neuron 1997;19:665–678. [PubMed: 9331356]

Hirono M, Konishi S, Yoshioka T. Phospholipase C-independent group I metabotropic glutamate receptor- mediated inward current in mouse purkinje cells. Biochem Biophys Res Commun 1998;251:753–758. [PubMed: 9790982]

Ichise T, Kano M, Hashimoto K, Yanagihara D, Nakao K, Shigemoto R, Katsuki M, Aiba A. mGluR1 in cerebellar Purkinje cells essential for long-term depression, synapse elimination, and motor coordination. Science 2000;288:1832–1835. [PubMed: 10846166]

Ito M. Cerebellar long-term depression: characterization, signal transduction, and functional roles. Physiol Rev 2001;81:1143–1195. [PubMed: 11427694]

Jorntell H, Ekerot CF. Reciprocal bidirectional plasticity of parallel fiber receptive fields in cerebellar Purkinje cells and their afferent interneurons. Neuron 2002;34:797–806. [PubMed: 12062025]

Kreitzer AC, Regehr WG. Retrograde signaling by endocannabinoids. Curr Opin Neurobiol 2002;12:324–330. [PubMed: 12049940]

Kreitzer AC, Carter AG, Regehr WG. Inhibition of interneuron firing extends the spread of endocannabinoid signaling in the cerebellum. Neuron 2002;34:787–796. [PubMed: 12062024]

Llano I, Marty A. Presynaptic metabotropic glutamatergic regulation of inhibitory synapses in rat cerebellar slices. J Physiol 1995;486:163–176. [PubMed: 7562633]

Lujan R, Nusser Z, Roberts JD, Shigemoto R, Somogyi P. Perisynaptic location of metabotropic glutamate receptors mGluR1 and mGluR5 on dendrites and dendritic spines in the rat hippocampus. Eur J Neurosci 1996;8:1488–1500. [PubMed: 8758956]

Maejima T, Hashimoto K, Yoshida T, Aiba A, Kano M. Presynaptic inhibition caused by retrograde signal from metabotropic glutamate to cannabinoid receptors. Neuron 2001;31:463–475. [PubMed: 11516402]

Negyessy L, Vidnyanszky Z, Kuhn R, Knopfel T, Gorcs TJ, Hamori J. Light and electron microscopic demonstration of mGluR5 metabotropic glutamate receptor immunoreactive neuronal elements in the rat cerebellar cortex. J Comp Neurol 1997;385:641–650. [PubMed: 9302110]

Nusser Z, Mulvihill E, Streit P, Somogyi P. Subsynaptic segregation of metabotropic and ionotropic glutamate receptors as revealed by immuno-gold localization. Neuroscience 1994;61:421–427. [PubMed: 7969918]

Otis TS, Kavanaugh MP, Jahr CE. Postsynaptic glutamate transport at the climbing fiber-Purkinje cell synapse. Science 1997;277:1515–1518. [PubMed: 9278516]

Palay, SL.; Chan-Palay, V. Cerebellar Cortex: Cytology and Organization. Springer-Verlag; New York: 1974.

Petralia RS, Wang YX, Singh S, Wu C, Shi L, Wei J, Wenthold RJ. A monoclonal antibody shows discrete cellular and subcellular localizations of mGluR1 alpha metabotropic glutamate receptors. J Chem Neuroanat 1997;13:77–93. [PubMed: 9285353]

Pin JP, Duvoisin R. The metabotropic glutamate receptors: structure and functions. Neuropharmacology 1995;34:1–26. [PubMed: 7623957]

Rancillac A, Crepel F. Synapses between parallel fibres and stellate cells express long-term changes in synaptic efficacy in rat cerebellum. J Physiol 2004;554:707–720. [PubMed: 14617674]

Sultan F, Bower JM. Quantitative Golgi study of the rat cerebellar molecular layer interneurons using principal component analysis. J Comp Neurol 1998;393:353–373. [PubMed: 9548555]

Takechi H, Eilers J, Konnerth A. A new class of synaptic response involving calcium release in dendritic spines. Nature 1998;396:757–760. [PubMed: 9874373]

Tempia F, Miniaci MC, Anchisi D, Strata P. Postsynaptic current mediated by metabotropic glutamate receptors in cerebellar Purkinje cells. J Neurophysiol 1998;80:520–528. [PubMed: 9705447]

Varma N, Carlson GC, Ledent C, Alger BE. Metabotropic glutamate receptors drive the endocannabinoid system in hippocampus. J Neurosci 2001;21:RC188. [PubMed: 11734603]

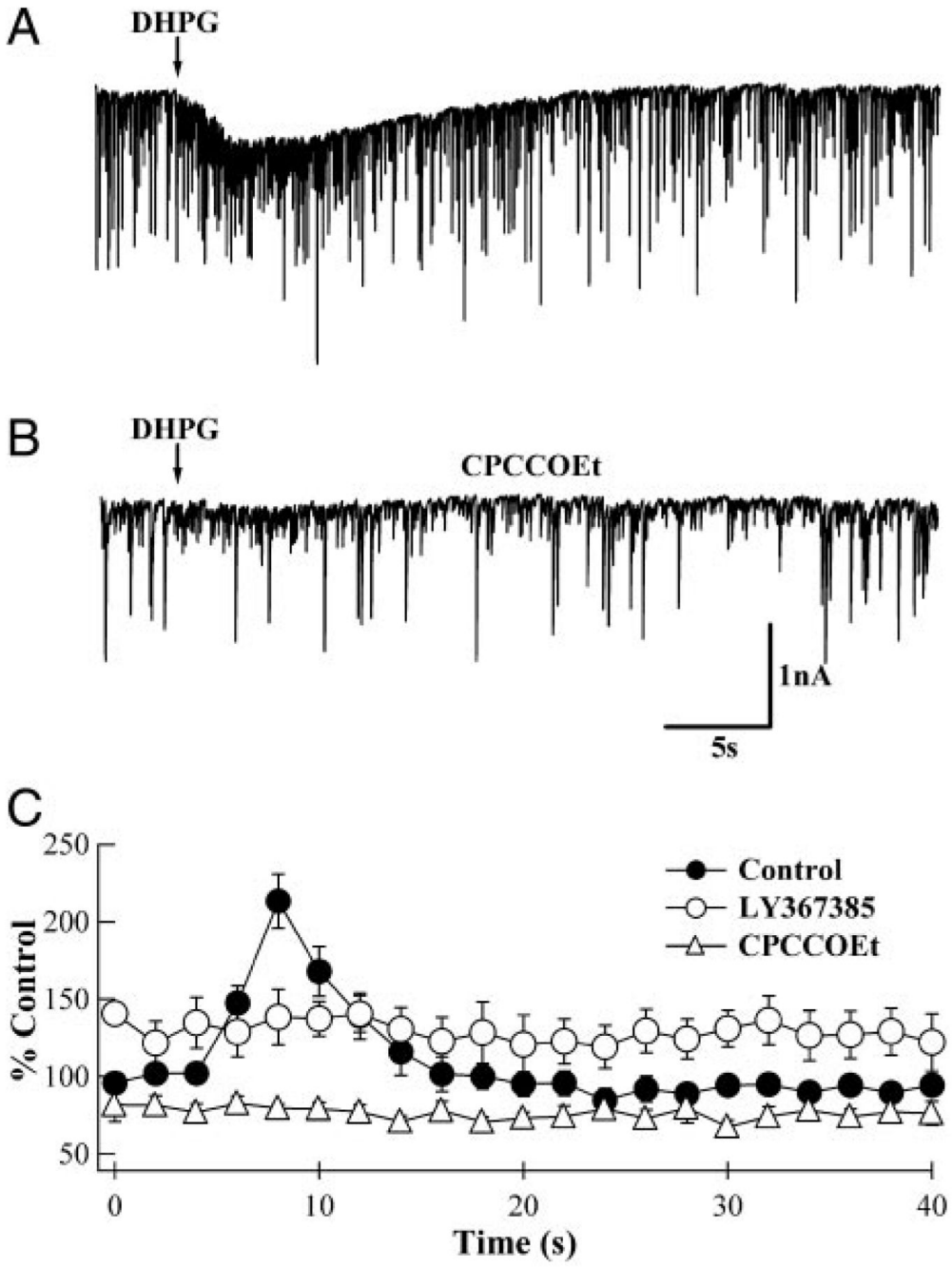

FIG. 1.

G-protein–coupled glutamate receptor (mGluR)-induced increases in spontaneous inhibitory postsynaptic current (sIPSC) frequency are inhibited by the specific mGluR1α antagonists, (*S*)-(+)-α-amino-4-carboxy-2-methylbenzeneacetic acid (LY367385) and 7-(hydroxyimino) cyclopropa[b]chromen-1a-carboxylate ethyl ester (CPCCOEt). *A*: whole cell recording from a Purkinje neuron (PN) indicating an increase in sIPSC frequency on pressure application of (*RS*)-3,5-dihydroxyphenylglycine (DHPG; arrow). *B*: same PN in the presence of 100 μM CPCCOEt shows no response to pressure application of DHPG. *C*: analyzed results from several recordings similar to those shown in *A* and *B*. Average frequencies from 2–3 responses from the same PN were calculated for 2-s bin sizes and normalized to values in the 1st 3 bins.

In the absence of mGluR1 antagonists (●), DHPG increased the sIPSC frequency to a peak of 213 ± 18% (n = 11; P < 0.01). In the presence of LY367385 (○), the baseline sIPSC frequency was elevated to 129 ± 15% (n = 5) of control, but did not change in response to the DHPG application (P = 0.78). In the presence of 100 μM CPCCOEt (△), although the baseline sIPSC frequency was reduced (76 ± 6%; n = 6), DHPG application had no effect on sIPSC frequency (P = 0.90). The timing of DHPG application has been synchronized with the arrows in *A* and *B*.

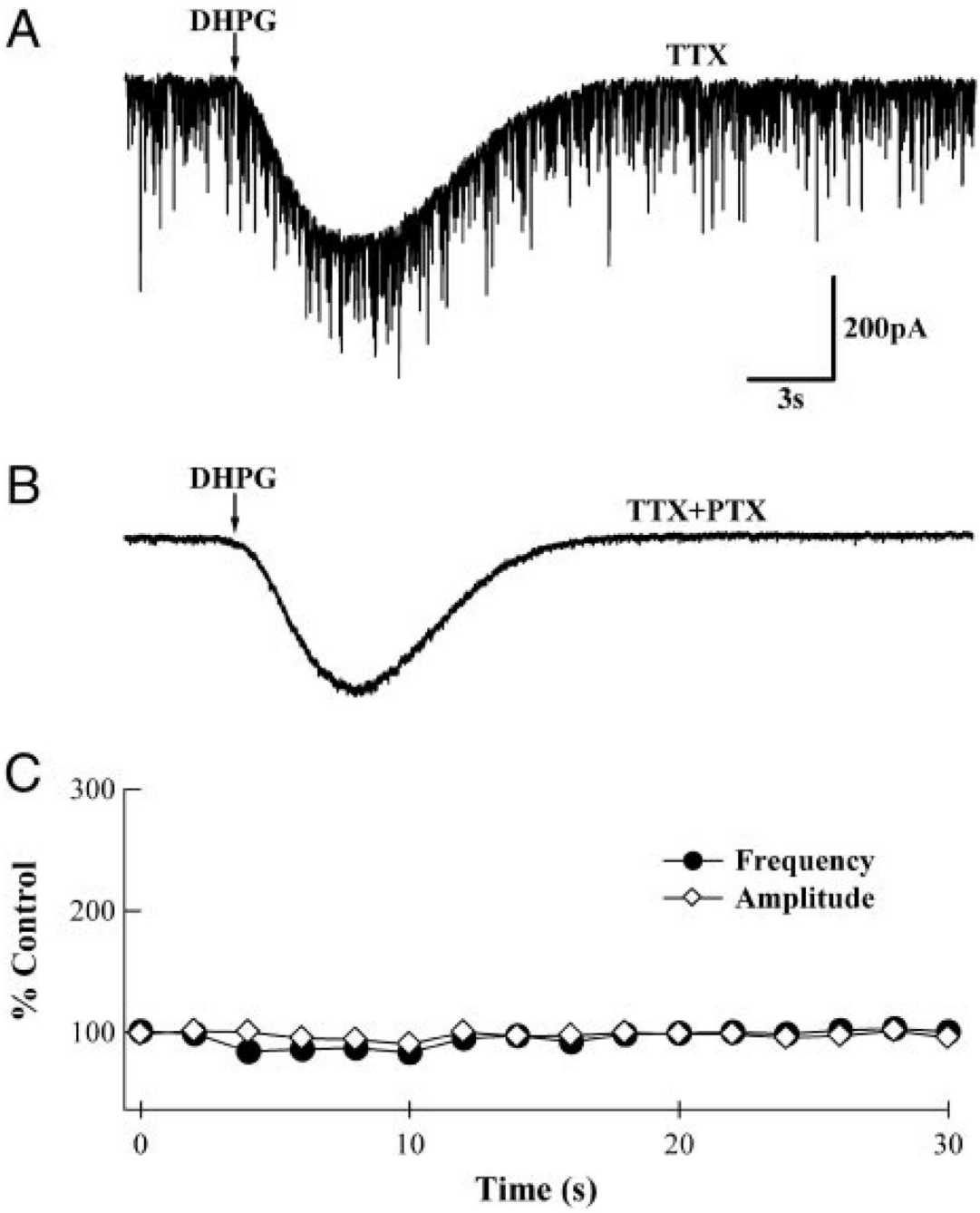

FIG. 2.

mGluR-induced IPSCs are GABAergic and presynaptic in origin. *A*: whole cell recording from a PN in the presence of 500 nM TTX and 100 μM $CdCl_2$. DHPG application gave rise to an mGluR excitatory postsynaptic potential (EPSC); however, no change in miniature (m)IPSC frequency was apparent. *B*: same PN in the presence of 100 μM picrotoxin (PTX). Note that mIPSCs are abolished, leaving the mGluR-activated inward current. *C*: analyzed results from 7 PNs show that DHPG does not elicit significant increases in mIPSC frequency or amplitude. Mean frequencies (●) and amplitudes (◇) were calculated for 2-s bins and normalized to values in the 1st 2 bins. Error bars are obscured by the symbols.

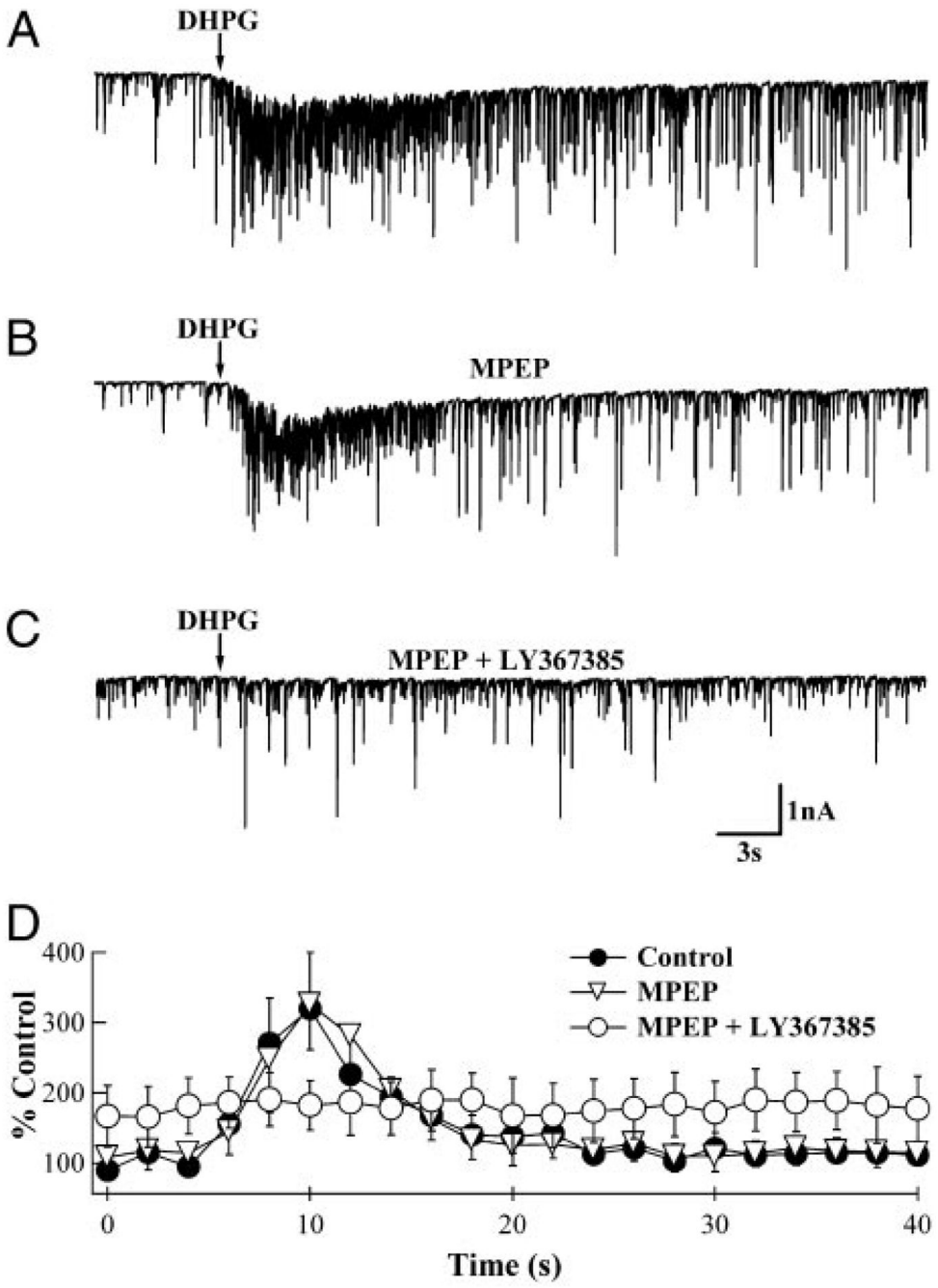

FIG. 3.

DHPG-induced high-frequency sIPSCs are not blocked by a specific mGluR5 antagonist. *A*: whole cell recording from a PN indicating an increase in sIPSC frequency by the pressure application of DHPG (arrow). *B*: similar response is observed in the same PN in the presence of the specific mGluR5 antagonist, 1 μM 2-methyl-6-[phenylethynyl]pyridine hydrochloride (MPEP). *C*: this DHPG-induced burst is abolished in the presence of LY367385 (100 μM). *D*: analyzed results from several recordings similar to those shown in *A*–*C*. Average frequencies from 2–3 responses from the same PN were calculated in 2-s bins and normalized. sIPSC frequency increased 319 ± 80% in the absence of antagonists (●) and 326 ± 64% in the presence of MPEP (▽; $n = 5$; $P = 0.95$). In the presence of LY367385 (○), DHPG application had no

effect on sIPSC frequency ($n = 5$; $P = 0.86$). Timing of DHPG application has been synchronized with the arrows in *A–C*.

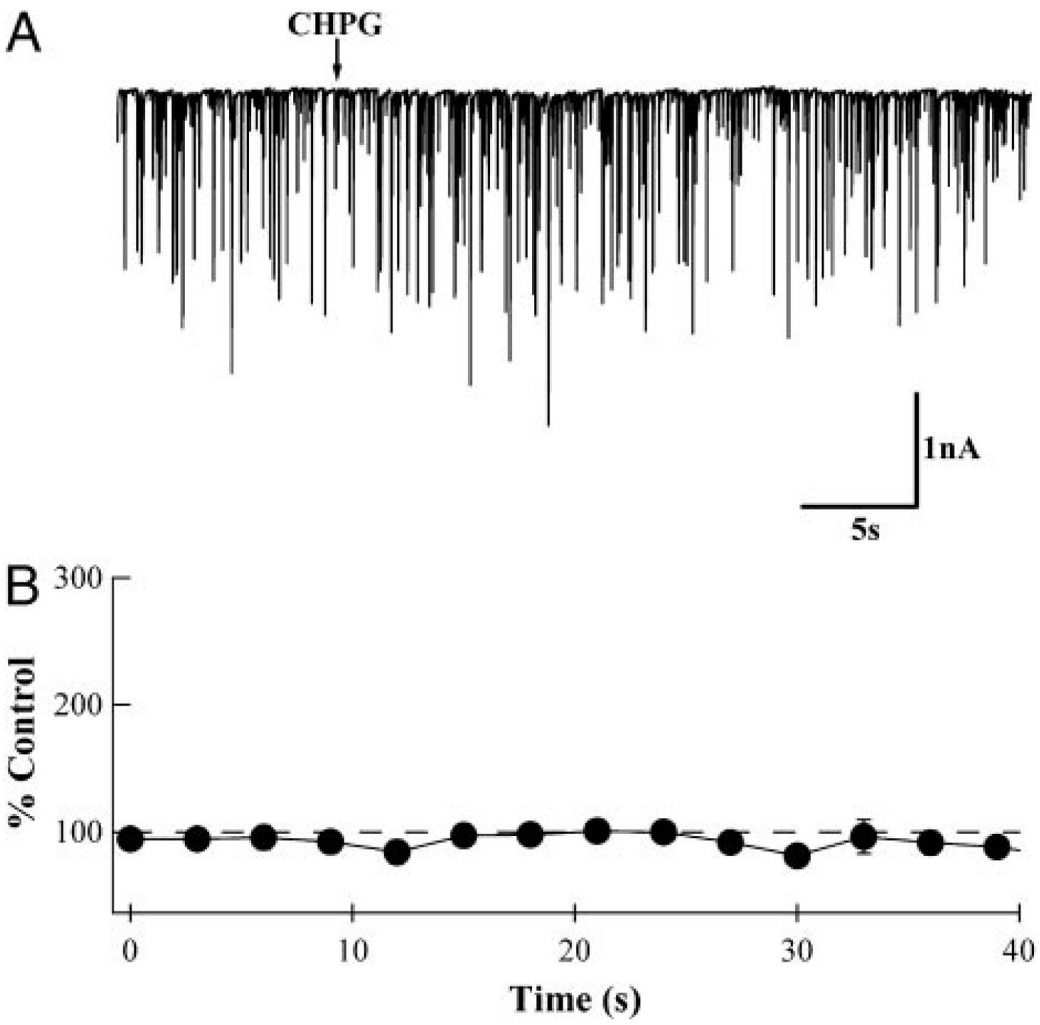

FIG. 4.

DHPG-induced high-frequency sIPSCs are not due to the activation of mGluR5. *A*: whole cell patch recording from a PN. Pressure application of 1 mM [*RS*]-2-chloro-5-hydroxyphenylglycine (CHPG; arrow), a specific mGluR5 agonist. *B*: analyzed results from 6 recordings similar to those shown in *A*. Average frequencies from 2–3 responses from the same PN were calculated for 3-s bins and normalized to values in the 1st 3 bins. CHPG application had no effect on sIPSC frequency ($P = 0.22$). The timing of CHPG application is synchronized with the arrow in A.

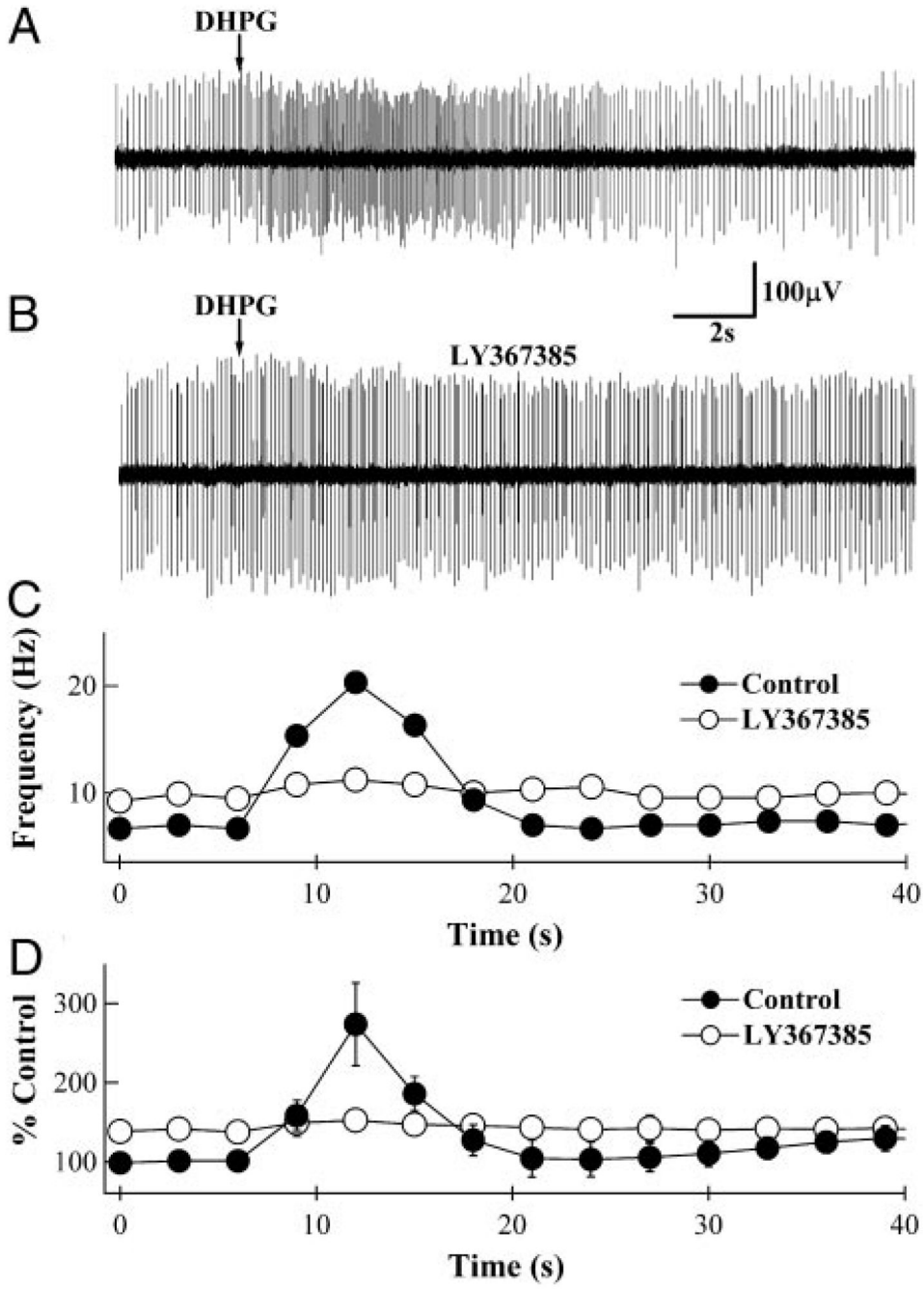

FIG. 5.

DHPG-induced high-frequency action potentials in basket and stel-late neurons (BSNs). *A*: loose-patch extracellular recording from a BSN, indicating an increase in action potential firing rate on pressure application of DHPG (arrow). *B*: increase in firing rate is absent in the presence of 100 μM LY367385. *C*: analyzed results from the recordings shown in *A* and *B*. Average frequencies for 2–3 responses from the same PN were measured and binned to 3 s. Timing of DHPG application has been synchronized with the arrows in *A* and *B*. In response to DHPG, action potential firing frequency in this cell transiently increased from 7 to 20 Hz (●), and this increase was blocked by LY367385 (○). Baseline frequency in LY367385 was slightly elevated to 10 Hz. *D*: normalized mean firing frequency vs. time obtained from several different BSNs.

Under control conditions (F), DHPG application transiently increased the firing frequency to 273 ± 52% (n = 6; P < 0.01). In the presence of LY367385 (○) the DHPG-induced increase was abolished, but the baseline firing frequency was elevated to 142 ± 14% (n = 6; P = 0.58) of control. Note the difference in the time scale of *A* and *B* compared with *C* and *D*.

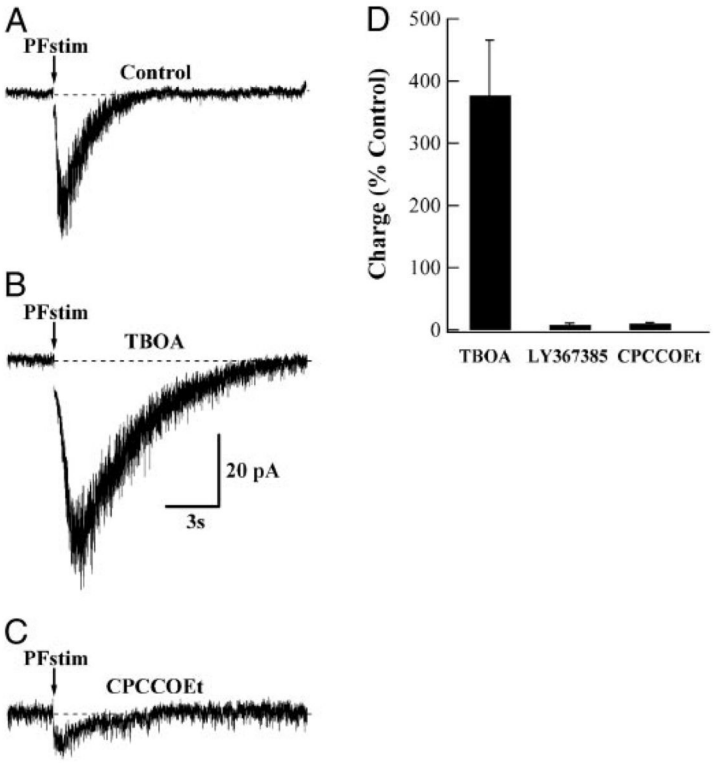

FIG. 6.

A synaptically evoked slow mGluR EPSC in BSNs. *A*: whole cell voltage-clamp recording from a BSN in the presence of $GABA_A$, AMPA, and *N*-methyl-D-aspartate (NMDA) receptor antagonists is displayed. At the arrow, a train of 10 stimuli at 100 Hz has been delivered to parallel fibers eliciting a slow inward current. *B*: response to an identical stimulus in the presence of the glutamate transporter antagonist D,L-*threo*-β-benzyloxyaspartate (TBOA; 100 μM) is markedly enhanced. *C*: bath application of the mGluR1*α* antagonist CPCCOEt (200 μM) significantly reduced the current. *D*: summary plot showing means ± SE of the mGluR EPSCs from several BSNs. In the presence of 100 μM TBOA, the mean charge integral of the current was enhanced to 377 ± 89% ($n = 11$; $P < 0.01$). In the presence of 200 μM LY367385 and CPCCOEt, the synaptically evoked charge integral of the current was reduced to 7.8 ± 3% ($n = 6$; $P = 0.01$) and 10.5 ± 1.6% ($n = 5$; $P = 0.02$), respectively, compared with TBOA. Antagonists were bath-applied in the presence of TBOA and were therefore normalized to measurements made in TBOA.

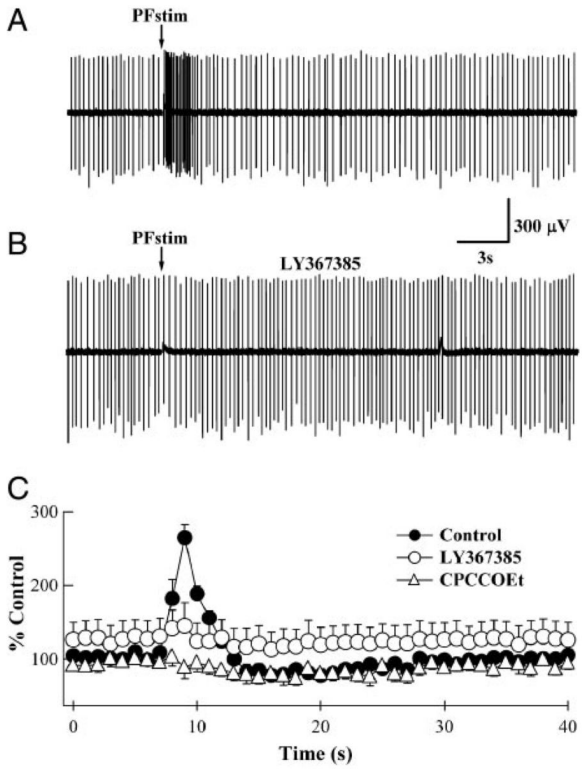

FIG. 7.

Synaptically activated high-frequency action potentials in BSNs. *A*: loose-patch extracellular recording from a BSN. A train of 10 stimuli at 100 Hz delivered to parallel fibers (arrow) in the presence of $GABA_A$, AMPA, and NMDA receptor antagonists resulted in a burst of action potentials. *B*: in the same BSN, 200 μM LY367385 prevented the synaptically evoked increase in firing rate. *C*: analyzed results from similar records shown in *A* and *B* and in the presence of CPCCOEt (raw trace not shown). Average frequencies from 2–3 responses from the same BSN were binned to 1 s and normalized. In the absence of antagonists (●), parallel fiber stimulation increased the baseline action potential frequency to 265 ± 18% ($n = 10$; $P < 0.01$). In the presence of LY367385 (○), the baseline firing frequency was elevated to 127 ± 24% of that measured in control BSNs, but did not significantly change in response to parallel fiber stimulation (145 ± 32%; $P = 0.62$). In the presence of 100 μM CPCCOEt (△), although the baseline action potential frequency was slightly reduced (92 ± 9%; $n = 6$; excluding 2 BSNs that reversibly but completely ceased firing in the presence of 100 μM CPCCOEt), parallel fiber stimulation had no effect on action potential frequency ($P = 0.63$). The timing of parallel fiber stimulation has been synchronized with the arrows in *A* and *B*.